Supplementary Information

Ratiometric Fluorescence Probe based on Dual-Ligand Lanthanide Metal-Organic Framework (MOF) for Sensitive Detection of Aluminium and Fluoride Ions in River and Tap Water

Runnan Wang[a,c], Hao Zhang[c], Sibo Wang[a], Fanxu Meng[d], Jing Sun[*,b], Dawei Lou[c], Zhongmin Su[*,b]

[a] *School of Materials science and Engineering, Changchun University of Science and Technology, Changchun,130022, People's Republic of China.*

[b] *School of Chemistry and Environmental Engineering, Changchun University of Science and Technology, Jilin Provincial Science and Technology Innovation Center of Optical Materials and Chemistry, Jilin Provincial International Joint Research Center of Photo functional Materials and Chemistry, Changchun, 130022, People's Republic of China.*

[c] *Department of Analytical Chemistry, Jilin Institute of chemical Technology, Financial support from the Key Laboratory of Fine Chemicals of Jilin Province is also acknowledged, Jilin, 132022, PR China.*

[d] *Center of Characterization and Analysis, Jilin Institute of Chemical Technology, Jilin, 132022, PR China.*

*correspondence: sj-cust@126.com; zmsu@nenu.edu.cn

Materials and measurement

2-Aminoterephthalic acid (BDC-NH_2), 2,5-Thiophenedicarboxylic acid (TDA) and N,N-Dimethylacetamide (DMA), Metal salts ($Eu(NO)_3 \cdot 6H_2O$, $Al(NO_3)_3 \cdot 9H_2O$, $Ca(NO_3)_2 \cdot 4H_2O$, $Cu(NO_3)_2 \cdot 2.5H_2O$, $Co(NO_3)_2 \cdot 6H_2O$, $Zn(NO_3)_2 \cdot 6H_2O$, $Fe(NO_3)_3 \cdot 9H_2O$, $Fe(NO_3)_2 \cdot 6H_2O$, $Ni(NO_3)_2 \cdot 6H_2O$, $Cr(NO_3)_3 \cdot 9H_2O$, KNO_3, $NaNO_3$, NH_4NO_3, $Pb(NO_3)_2 \cdot 3H_2O$, $Hg(NO_3)_2 \cdot 5H_2O$, $AgNO_3 \cdot 9H_2O$, KF, KCl, KBr and KI) were purchased from Aladdin BioChem Technology Co. Ltd. Shanghai, China. All the chemicals were commercially purchased and used without further purification.

Fluorescence spectrum analysises were performed on a HORIBA Fluoromax TCSPC fluorescence spectrometer. Powder X-ray diffraction (XRD) of the MOF samples were performed by using a Bruker D8 apparatus equipped with Cu kα radiation and recorded in the 2θ range of 5−60° under room conditions. The simulated powder patterns of Eu-BDC-NH_2/TDA were calculated using Mercury 3.8 via CIF files. A Thermo Fisher Scientific Cahn thermogravimetric analyzer apparatus was implemented with a heating rate of 5 °C/min from room temperature to 800 °C under a N_2 atmosphere to determine the TGA curves of the MOF. Fourier transform infrared (FT-IR) spectroscopy was conducted on a Thermo Fisher Scientific Nicolet iS 50 spectrometer in the range of 4000-400 cm^{-1} with a powder sample on a KBr pellets. X-ray photoelectron spectra (XPS) was collected on a Thermo Fisher Scientific ESCALAB 250XI device. N_2 adsorption-desorption isotherms were carried out by Micromeritics ASAP2020. The single crystal X-ray was measured on a Bruker APEX-II CCD diffractometer with graphite monochromatic Mo Ka radiation at 298 K, and the structure was solved by direct method and refined with the full matrix least-squares method on F2 embedded in SHELXTL program through using the Olex2 as the graphical interface. All hydrogen atoms were placed geometrically in ideal positions with a riding model, and all non-hydrogen atoms were refined by the anisotropic thermal parameters during the final cycles.

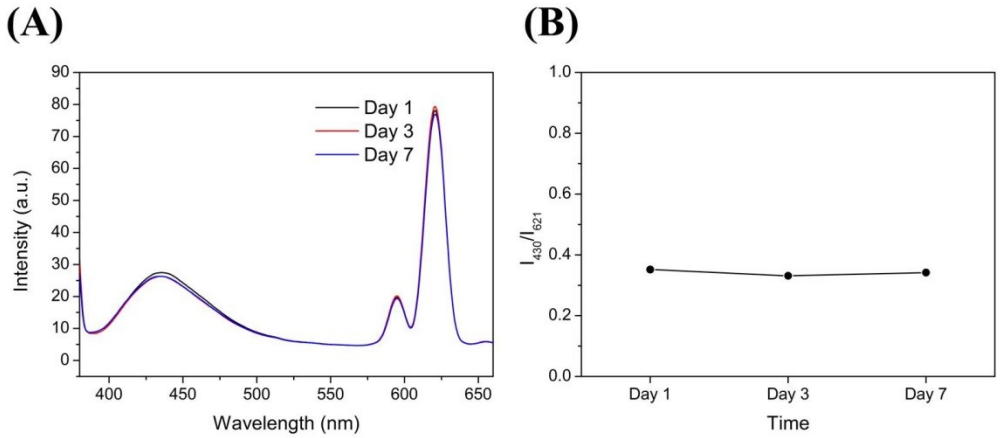

Fig.S1. (A) Fluorescence spectra and the fluorescence intensity ratio of I_{430}/I_{621} (B) of Eu-BDC-NH_2/TDA stored in room temperature within seven days.

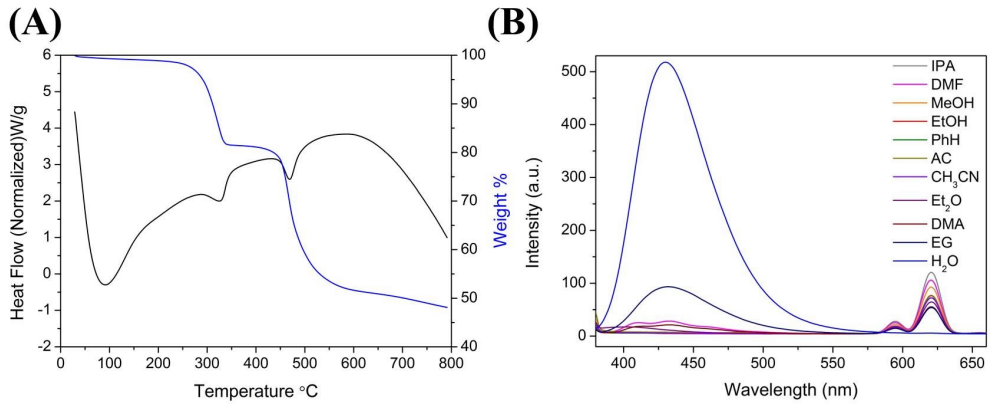

Fig.S2. (A) Thermogravimetric analysis of Eu-BDC-NH_2/TDA. (B) Luminescence intensity of Eu-BDC-NH_2/TDA dispersed in different solvents.

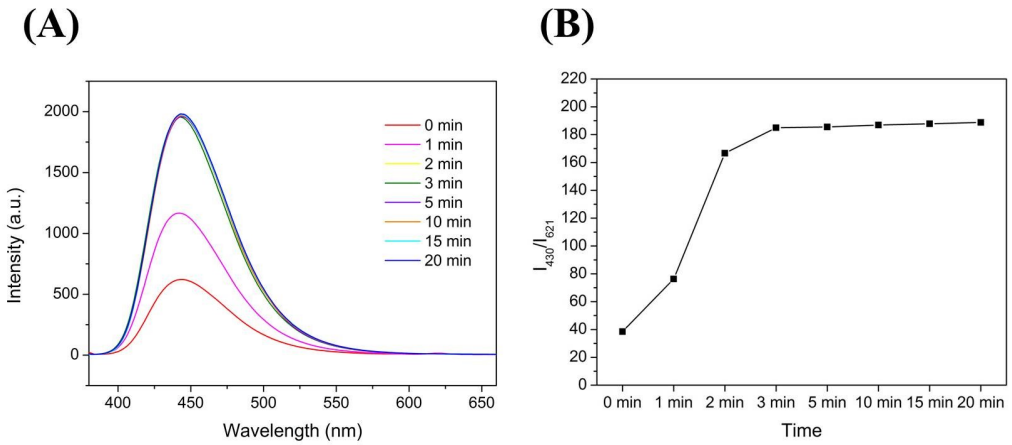

Fig.S3. (A) Fluorescence spectra and the fluorescence intensity ratio of I_{430}/I_{621} (B) of Eu-BDC-NH_2/TDA towards Al^{3+} at different response time.

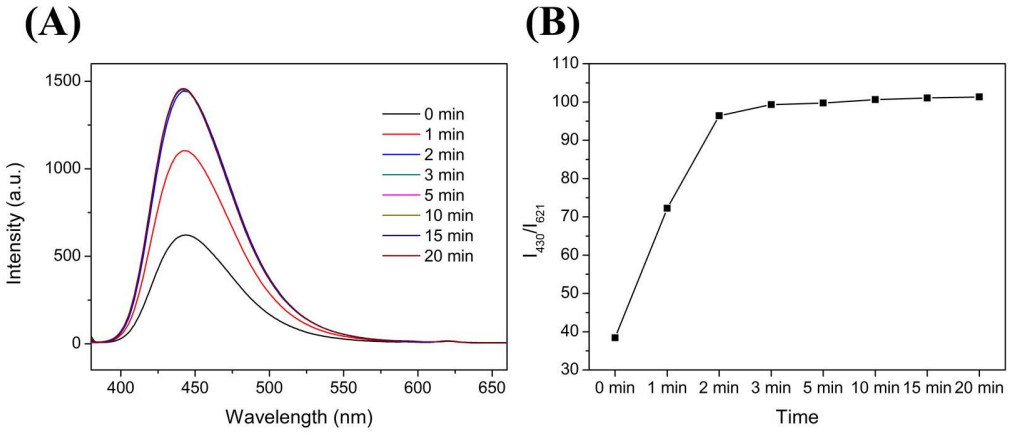

Fig.S4. (A) Fluorescence spectra and the fluorescence intensity ratio of I_{430}/I_{621} (B) of Eu-BDC-NH_2/TDA towards F^- at different response time.

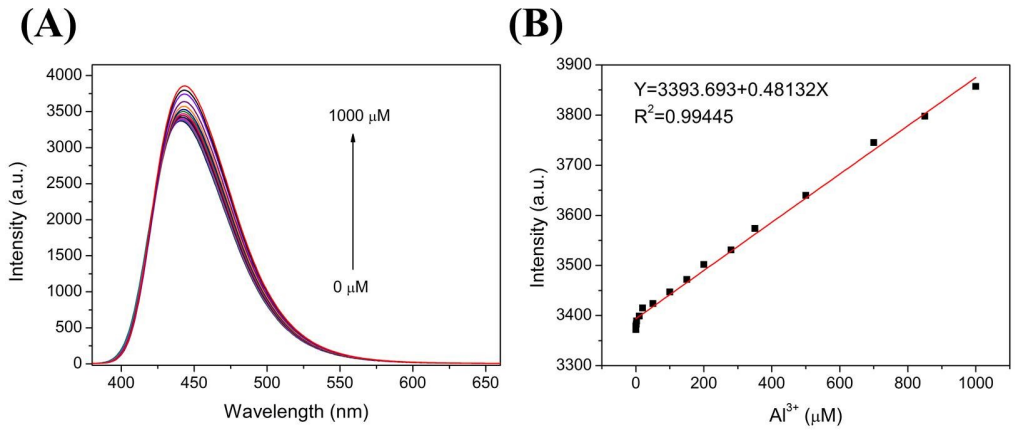

Fig.S5. (A) Fluorescence emission spectra of BDC-NH_2 in the presence of different concentrations of Al^{3+}. (B) Linear relationship between the I_{430}/I_{621} and concentration of Al^{3+} in the range of 0–1000 μM.

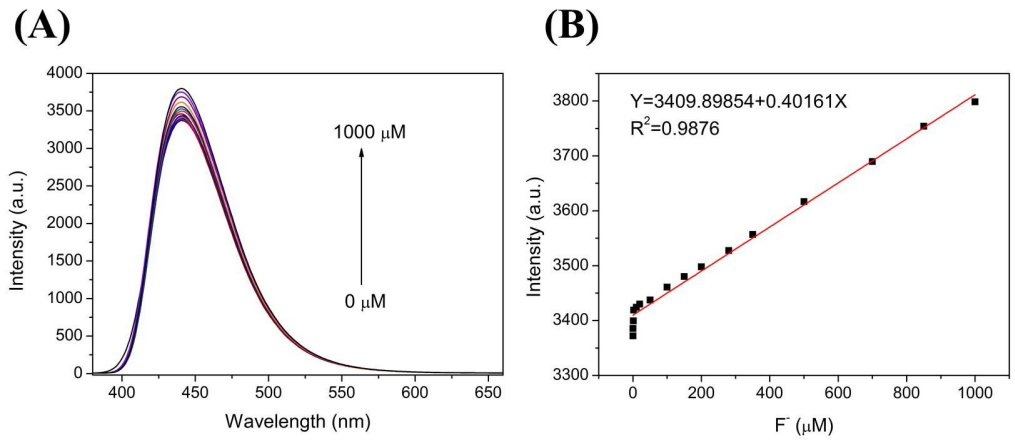

Fig.S6. (A) Fluorescence emission spectra of BDC-NH_2 in the presence of different concentrations of F^-. (B) Linear relationship between the I_{430}/I_{621} and concentration of F^- in the range of 0–1000 μM.

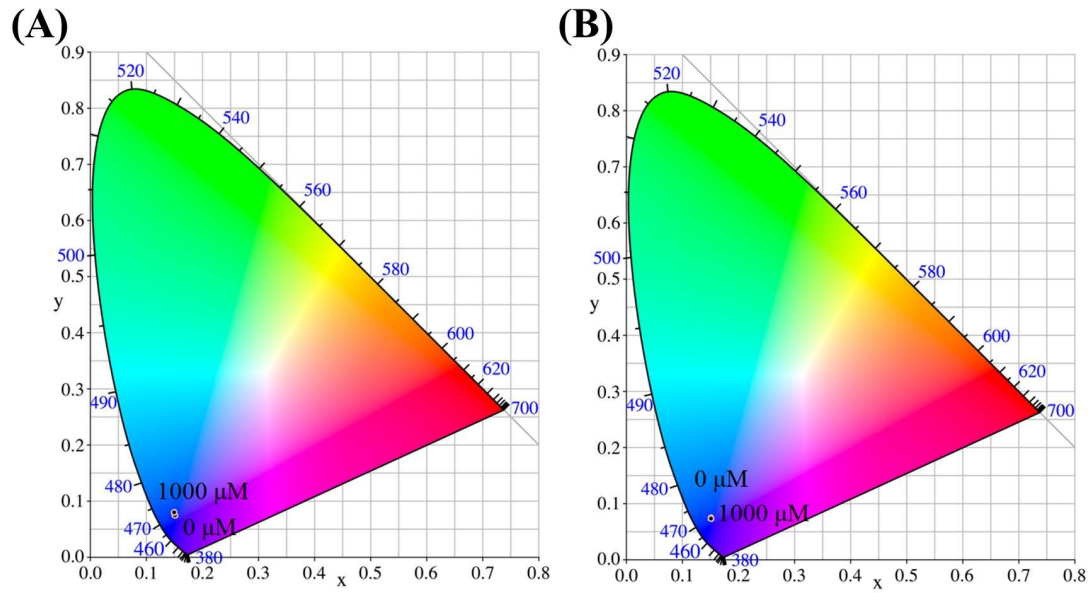

Fig.S7. (A) CIE chromaticity diagram of BDC-NH_2 in the presence of different concentrations of Al^{3+} and F^- (B) from 0 to 1000 μM.

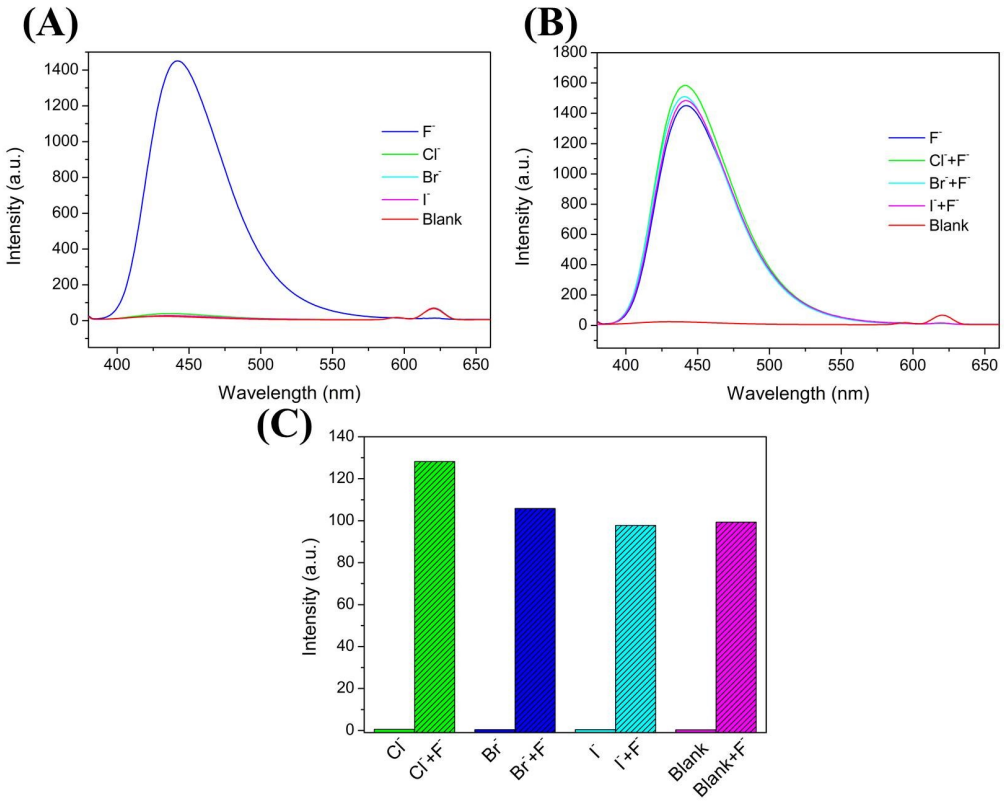

Fig.S8. (A) The fluorescence of Eu-BDC-NH_2/TDA responding to different halide ion. (B) The fluorescence of Eu-BDC-NH_2/TDA responding to F^- with other different halide ion as the interference. (C) The fluorescence intensity of I_{430}/I_{621} of Eu-BDC-NH_2/TDA and treated with various halide ion and the coexistence of F^-.

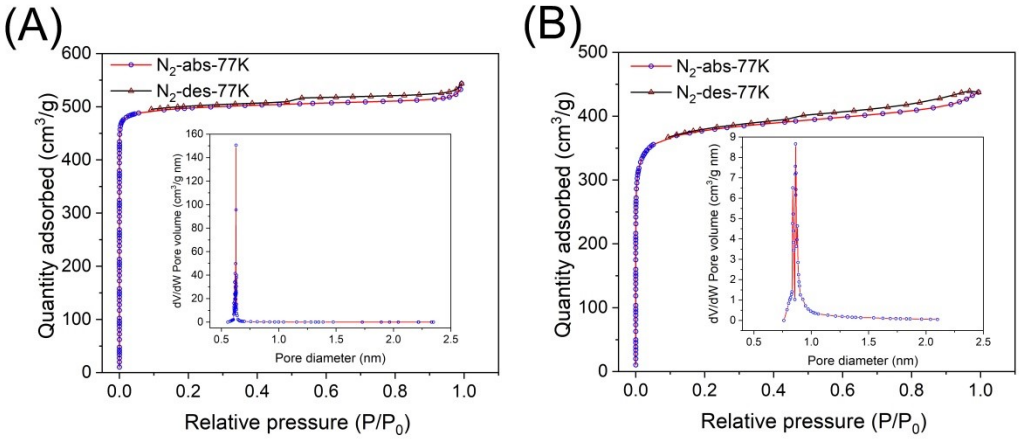

Fig.S9. (A) N_2 adsorption-desorption isotherms of Eu-BDC-NH_2/TDA and (B) Al@Eu-BDC-NH_2/TDA. Inset: the pore size distributions.

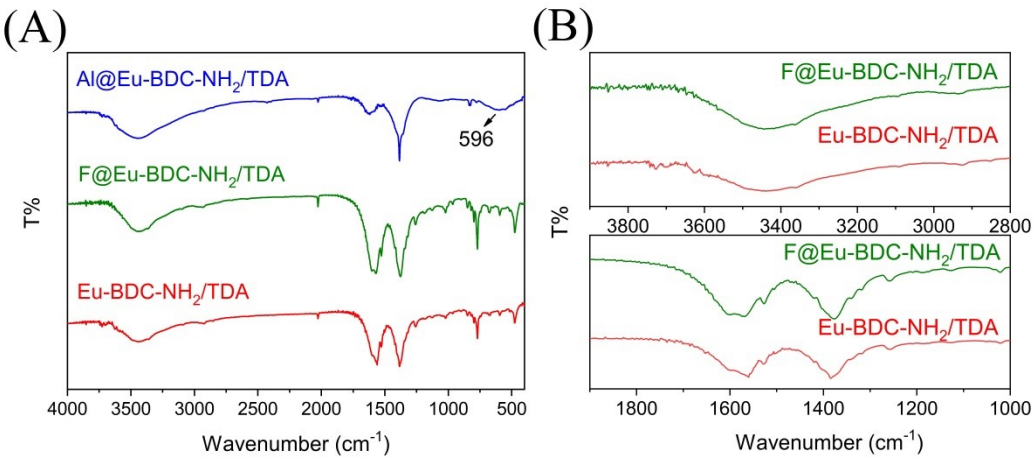

Fig.S10. FT-IR spectra of Eu-BDC-NH_2/TDA, Al@Eu-BDC-NH_2/TDA and F@Eu-BDC-NH_2/TDA.

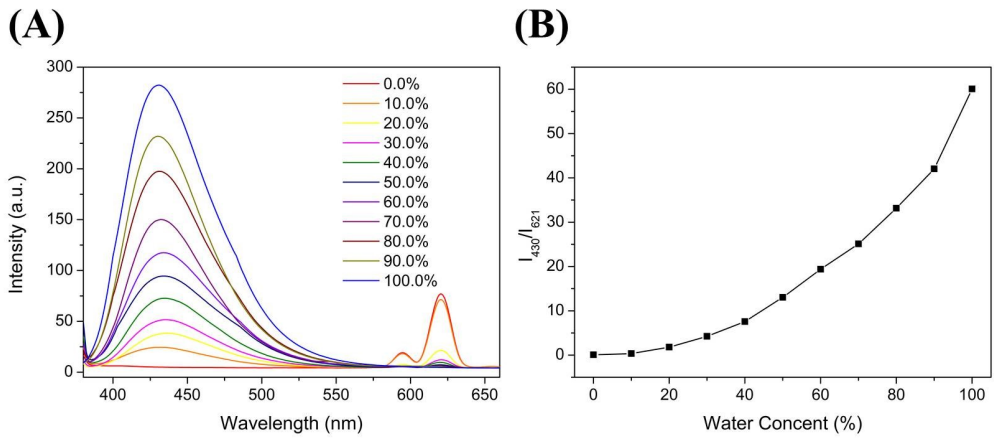

Fig.S11. (A) Emission spectra of Eu-BDC-NH_2/TDA in ethanol with different content of water. (B) Change of the I_{430}/I_{621} upon the increase of water concentration.

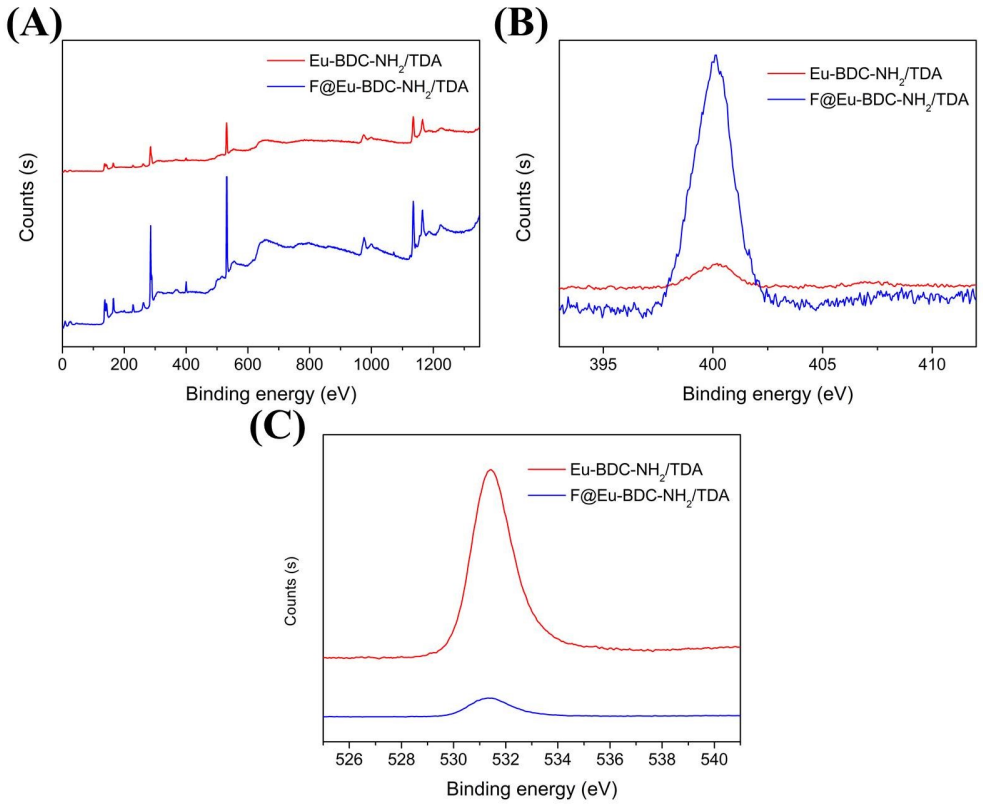

Fig. S12. (A) XPS spectra for Eu-BDC-NH_2/TDA and F@Eu-BDC-NH_2/TDA. (B) XPS spectra for N 1s in Eu-BDC-NH_2/TDA and F@Eu-BDC-NH_2/TDA. (C) XPS spectra for O 1s in Eu-BDC-NH_2/TDA and F@Eu-BDC-NH_2/TDA.

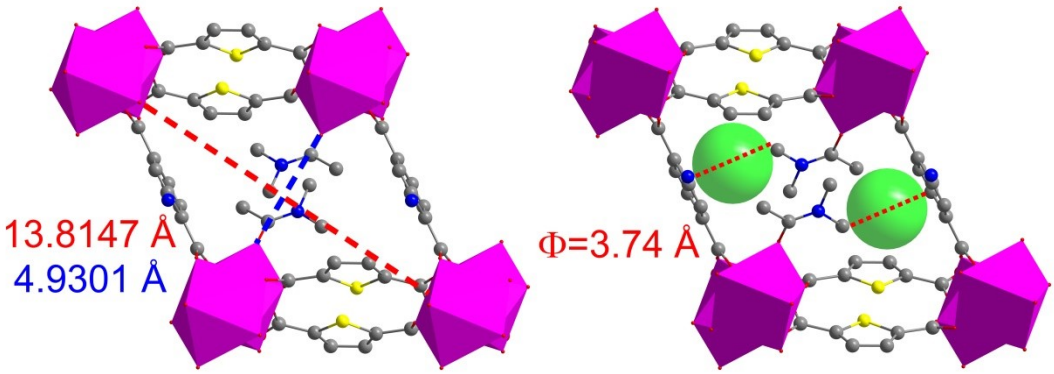

Fig. S13. The schematic diagram of the aperture measurement of Eu-BDC-NH_2/TDA

Table S1 Crystal data and structure refinement for Eu-BDC-NH_2/TDA

Empirical formula	$C_{14}H_{13}EuN_{1.5}O_7S$
Formula weight	498.28
Temperature/K	296.15
Crystal system	triclinic
Space group	P-1
a/Å	8.967(6)
b/Å	10.323(7)

c/Å	10.471(7)
α/°	115.226(8)
β/°	91.750(8)
γ/°	109.208(8)
Volume/Å^3	811.4(10)
Z	2
ρ_{calc}g/cm^3	2.040
μ/mm^{-1}	4.032
F(000)	485.0
Radiation	MoKα (λ = 0.71073)
2Θ range for data collection/°	4.388 to 55.254
Index ranges	-11 ≤ h ≤ 11, -8 ≤ k ≤ 13, -13 ≤ l ≤ 13
Reflections collected	4664
Independent reflections	3628 [R_{int} = 0.0242, R_{sigma} = 0.0572]
Data/restraints/parameters	3628/22/230
Goodness-of-fit on F^2	1.054
Final R indexes [I>=2σ (I)]	R_1 = 0.0450, wR_2 = 0.1095
Final R indexes [all data]	R_1 = 0.0570, wR_2 = 0.1162
Largest diff. peak/hole / e Å^{-3}	2.16/-1.03

Table S2. Bond lengths [Å] and angles [°] for compound Eu-BDC-NH_2/TDA

Atom	**Atom**	**Length/Å**
Eu1	Eu1#1	4.047(2)
Eu1	O1#2	2.381(5)
Eu1	O2#3	2.381(5)
Eu1	O3#4	2.358(5)
Eu1	O4	2.311(5)
Eu1	O4#1	2.877(6)
Eu1	O5#1	2.389(6)
Eu1	O6	2.372(6)
Eu1	O7	2.286(6)
Eu1	C2#1	3.018(8)
S1	C3	1.710(7)
S1	C4	1.710(7)
O1	C1	1.254(9)
O2	C1	1.246(9)
O3	C6	1.237(9)
O4	C2	1.261(9)
O5	C2	1.249(10)
O6	C12	1.259(13)

Atom	Atom	Length/Å
O7	C6	1.278(10)
C1	C4	1.485(9)
C2	C8	1.461(10)
C3	C6	1.476(10)
C3	C7	1.361(11)
C4	C5	1.367(10)
C5	C7	1.390(10)
N1	C9	1.451(12)
N1	C10	1.493(14)
N1	C12	1.259(14)
C8	C13	1.3949(12)
C8	C14	1.3948(13)
C11	C12	1.567(18)
C13	C14#5	1.059(14)
C13	N2	1.37(3)

#1:1-X,-Y,1-Z; **#2:**1-X,1-Y,1-Z; **#3:** +X,-1+Y,+Z; **#4:**-X,-Y,1-Z; **#5:**1-X,-Y,2-Z

Table S3 Angles [°] for compound Eu-BDC-NH_2/TDA

Atom	Atom	Atom	Angle/°
O1#1	Eu1	Eu1#2	66.35(14)
O1#1	Eu1	O4#2	64.07(17)
O1#1	Eu1	O5#2	79.8(2)
O1#1	Eu1	C2#2	69.25(19)
O2#3	Eu1	Eu1#2	66.00(13)
O2#3	Eu1	O1#1	128.94(19)
O2#3	Eu1	O4#2	66.38(17)
O2#3	Eu1	O5#2	76.1(2)
O2#3	Eu1	C2#2	71.08(19)
O3#4	Eu1	Eu1#2	120.06(15)
O3#4	Eu1	O1#1	149.6(2)
O3#4	Eu1	O2#3	73.75(19)
O3#4	Eu1	O4#2	139.31(18)
O3#4	Eu1	O5#2	129.3(2)
O3#4	Eu1	O6	76.3(2)
O3#4	Eu1	C2#2	140.8(2)
O4	Eu1	Eu1#2	44.06(16)
O4#2	Eu1	Eu1#2	33.95(11)
O4	Eu1	O1#1	80.9(2)
O4	Eu1	O2#3	77.68(19)
O4	Eu1	O3#4	86.2(2)

Atom	Atom	Atom	Angle/°
O4	Eu1	O4#2	78.0(2)
O4	Eu1	O5#2	125.4(2)
O4	Eu1	O6	83.7(2)
O4#2	Eu1	C2#2	24.54(18)
O4	Eu1	C2#2	102.5(2)
O5#2	Eu1	Eu1#2	81.46(15)
O5#2	Eu1	O4#2	47.64(18)
O5#2	Eu1	C2#2	23.2(2)
O6	Eu1	Eu1#2	117.36(16)
O6	Eu1	O1#1	75.1(2)
O6	Eu1	O2#3	145.5(2)
O6	Eu1	O4#2	137.24(18)
O6	Eu1	O5#2	137.6(2)
O6	Eu1	C2#2	142.1(2)
O7	Eu1	Eu1#2	149.66(17)
O7	Eu1	O1#1	93.6(2)
O7	Eu1	O2#3	120.0(2)
O7	Eu1	O3#4	88.9(2)
O7	Eu1	O4#2	117.5(2)
O7	Eu1	O4	159.4(2)
O7	Eu1	O5#2	72.3(2)
O7	Eu1	O6	75.7(2)
O7	Eu1	C2#2	93.9(2)
C2#2	Eu1	Eu1#2	58.48(15)
C4	S1	C3	92.7(4)
C1	O1	Eu1#1	135.4(5)
C1	O2	Eu1#5	132.0(4)
C6	O3	Eu1#4	135.8(5)
Eu1	O4	Eu1#2	102.0(2)
C2	O4	Eu1#2	84.0(5)
C2	O4	Eu1	173.6(6)
C2	O5	Eu1#2	108.0(5)
C12	O6	Eu1	147.8(7)
C6	O7	Eu1	147.7(6)
O1	C1	C4	115.6(7)
O2	C1	O1	127.4(7)
O2	C1	C4	116.9(6)
O4	C2	Eu1#2	71.5(4)
O4	C2	C8	121.0(8)

Atom	Atom	Atom	Angle/°
O5	C2	Eu1#2	48.9(4)
O5	C2	O4	120.0(7)
O5	C2	C8	119.0(7)
C8	C2	Eu1#2	166.5(6)
C6	C3	S1	122.3(6)
C7	C3	S1	110.7(5)
C7	C3	C6	126.3(7)
C1	C4	S1	122.5(5)
C5	C4	S1	109.7(5)
C5	C4	C1	127.7(7)
C4	C5	C7	114.1(7)
O3	C6	O7	125.6(7)
O3	C6	C3	118.0(7)
O7	C6	C3	116.4(7)
C3	C7	C5	112.8(7)
C9	N1	C10	118.2(9)
C12	N1	C9	126.1(12)
C12	N1	C10	115.4(10)
C13	C8	C2	129.3(9)
C14	C8	C2	122.9(9)
C14	C8	C13	107.8(9)
O6	C12	C11	120.3(10)
N1	C12	O6	123.8(13)
N1	C12	C11	115.8(11)
C14#6	C13	C8	128.0(14)
C14#6	C13	N2	118.3(12)
N2	C13	C8	113.6(13)
C13#6	C14	C8	124.1(15)

#1:1-X,1-Y,1-Z; **#2:**1-X,-Y,1-Z; **#3:**+X,-1+Y,+Z; **#4:**-X,-Y,1-Z; **#5:**+X,1+Y,+Z; **#6:**1-X,-Y,2-Z